Convergence of a Pseudospectral Method for Optimal Control of Complex Dynamical Systems

Justin Ruths, Anatoly Zlotnik, and Jr-Shin Li

***Abstract*— Pseudospectral approximation techniques have been shown to provide effective and flexible methods for solving optimal control problems in a variety of applications. In this paper, we provide the conditions for the convergence of the pseudospectral method for general nonlinear optimal control problems. Further, we show that this proof is directly extendible to the multidimensional pseudospectral method for optimal ensemble control of a class of parameterized dynamical systems. Examples from quantum control and neuroscience are included to demonstrate the method.**

I. INTRODUCTION

Optimal control is a systematic and powerful approach to characterize a wide variety of problems arising in all areas of science and engineering. Many computational methods have been developed to solve these challenging problems. In the past two decades, a pseudospectral method for discretizing a continuous-time optimal control problem into a finite dimensional constrained nonlinear optimization has garnered significant interest and found application in research ranging from the design of satellite maneuvers [1] to the control of quantum phenomena [2]. In addition, a multidimensional extension has been developed to apply these methods to parameterized families of dynamical systems, arising in such areas as quantum control and neuroscience [3], [4], [5]. Despite widespread use, only recently has the literature addressed the important topic of convergence of the pseudospectral method.

Substantial work, including proof of convergence and the corresponding rates, has been done for systems that belong to the class of feedback linearizable form [6]. As there are many systems that do not conform to this specialized dynamics - for example, ensemble systems, as described in Section VI, do not belong to this category - analysis for general systems is of keen interest. Gong et al. have also shown major components of convergence with regard to general systems, including the convergence of the dual problem [1]. Here we extend these results and relax the necessary assumptions. In particular, we use results from polynomial approximation theory to make the proof more transparent and touch upon the convergence of the multidimensional extension.

This work was supported by the NSF Career Award #0747877 and the AFOSR YIP FA9550-10-1-0146

J. Ruths is with the Faculty of Engineering Systems & Design, Singapore University of Technology & Design, Singapore justinruths@sutd.edu.sg

A. Zlotnik is with the Department of Electrical & Systems Engineering, Washington University in Saint Louis, Saint Louis, MO 63112, USA azlotnik@ese.wustl.edu

J.-S. Li is with the Faculty of Electrical & Systems Engineering, Washington University in Saint Louis jsli@seas.wustl.edu

We briefly introduce a standard optimal control problem and review the pseudospectral method to provide a foundation for the proof. Several useful preliminary results are developed before we present the main result in section V. We then discuss the multidimensional extension for the pseudospectral method and comment on the convergence in section VI. We conclude by showing illustrative examples from quantum control and neuroscience.

II. PROBLEM STATEMENT

Without loss of generality, we consider an optimal control problem defined on the time interval $\Omega = [-1, 1]$.

Problem 1 (Continuous-Time Optimal Control):

$$\min \quad J(x,u) = \varphi(x(1)) + \int_{-1}^{1} \mathcal{L}(t, x(t), u(t))dt, \tag{1}$$

$$\text{s.t.} \quad \dot{x}(t) = f(x(t), u(t)), \tag{2}$$

$$e(x(-1), x(1)) = 0, \tag{3}$$

$$g(x(t), u(t)) \leq 0, \tag{4}$$

$$\|u(t)\| \leq A, \quad u \in H_m^\alpha(\Omega),\ \alpha > 2 \tag{5}$$

where $\varphi \in C^0$ is the terminal cost; the running cost, $\mathcal{L} \in C^\alpha$, where C^α is the space of continuous functions with α classical derivatives, and dynamics, $f \in C_n^{\alpha-1}$, where $C_n^{\alpha-1}$ is the space of n-vector valued $C^{\alpha-1}$ functions, with respect to its arguments the state, $x(t) \in \mathbb{R}^n$, and control, $u(t) \in \mathbb{R}^m$; e and g are terminal and path constraints, respectively; $H_m^\alpha(\Omega)$ is the m-vector valued Sobolev space. The norm associated with the Sobolev space with $m = 1$, $H^\alpha(\Omega)$, is given with respect to the $L^2(\Omega)$ norm,

$$\|h\|_{(\alpha)} = \left(\sum_{k=0}^{\alpha} \left|\left|h^{(k)}\right|\right|_2^2 \right)^{1/2}.$$

An optimal nonlinear control problem of this form is, in general, intractable and difficult to solve analytically. Here we use a direct collocation approach based on pseudospectral approximations to discretize this problem into a finite dimensional constrained nonlinear optimization. In the following section we review the key concepts of the pseudospectral method for optimal control.

III. PSEUDOSPECTRAL METHOD

As a collocation (interpolation) method, the pseudospectral method uses Lagrange polynomials to approximate the states and controls of the optimal control problem,

$$x(t) \approx \mathcal{I}_N x(t) = \textstyle\sum_{k=0}^{N} \bar{x}_k \ell_k(t), \tag{6}$$

$$u(t) \approx \mathcal{I}_N u(t) = \textstyle\sum_{k=0}^{N} \bar{u}_k \ell_k(t), \tag{7}$$

where $x(t_k) = I_N x(t_k) = \bar{x}_k$ and $u(t_k) = I_N u(t_k) = \bar{u}_k$ because the Lagrange polynomials have the property $\ell_k(t_i) = \delta_{ki}$, where δ_{ki} is the Kronecker delta function and t_k are the interpolation nodes [7]. Therefore, $\bar{x}_k$ and $\bar{u}_k$ are the discretized values of the original problem and become the decision variables of the subsequent discrete problem.

Although interpolating with Lagrange polynomials discretizes Problem 1, we need to ensure that the integral in (1) is computed accurately and the dynamics in (2) are obeyed. The integral can be approximated through Gauss quadrature; here we use Legendre polynomials as the orthogonal basis for the pseudospectral method. The Legendre-Gauss-Lobatto (LGL) quadrature approximation,

$$\int_{-1}^{1} f(t)dt \approx \sum_{i=1}^{N} f(t_i)w_i, \qquad w_i = \int_{-1}^{1} \ell_i(t)dt, \tag{8}$$

is exact if the integrand $f \in \mathbb{P}_{2N-1}$ and the nodes $t_i \in \Gamma^{LGL}$, where $\mathbb{P}_{2N-1}$ denotes the set of polynomials of degree at most $2N-1$ and where $\Gamma^{LGL} = \{t_i : \dot{L}_N(t)|_{t_i} = 0, i = 1, \dots N-1\} \bigcup \{-1, 1\}$ are the $N+1$ LGL nodes determined by the derivative of the N^{th} order Legendre polynomial, $\dot{L}_N(t)$, and the interval endpoints [8].

Using the LGL nodes, we can rewrite the Lagrange polynomials in terms of the orthogonal Legendre polynomials. This is critical for the approximation to inherit the special derivative and spectral accuracy properties of orthogonal polynomials, despite the use of Lagrange interpolating polynomials. Given $t_k \in \Gamma^{LGL}$, we can express the Lagrange polynomials as [9],

$$\ell_k(t) = \frac{1}{N(N+1)L_N(t_k)} \frac{(t^2-1)\dot{L}_N(t)}{t-t_k}.$$

The derivative of (6) at $t_j \in \Gamma^{LGL}$ is then,

$$\frac{d}{dt} I_N x(t_j) = \sum_{k=0}^{N} \bar{x}_k \dot{\ell}_k(t_j) = \sum_{k=0}^{N} D_{jk}\bar{x}_k \triangleq (\mathcal{D}_N x)(t_j), \tag{9}$$

where D is the constant differentiation matrix [8].

We are now able to write the discretized optimal control problem using equations (6), (7), (8), and (9). We transform the continuous-time problem to a constrained optimization.

Problem 2 (Algebraic Nonlinear Programming):

$$\min \quad \bar{J}(\bar{x}, \bar{u}) = \varphi(\bar{x}_N) + \sum_{k=0}^{N} \mathcal{L}(\bar{x}_k, \bar{u}_k) w_k \tag{10}$$

$$\text{s.t.} \quad \big|\big| f(\mathcal{I}_N x, \mathcal{I}_N u) - \mathcal{D}_N x \big|\big|_N \le c_d N^{1-\alpha} \tag{11}$$

$$e(\bar{x}_0, \bar{x}_N) = 0 \tag{12}$$

$$g(\bar{x}_k, \bar{u}_k) \le 0 \tag{13}$$

$$\|u_k\| \le A \quad \forall\ k = 0, 1, \dots, N \tag{14}$$

where c_d is a positive constant; we define the discrete $L_n^2(\Omega)$ norm $\|h\|_N = \sqrt{\langle h, h\rangle_N}$, for $h, h_1, h_2 \in L_n^2(\Omega)$, with

$$\langle h_1, h_2 \rangle_N = \sum_{k=0}^{N} h_1^T(t_k) h_2(t_k) w_k.$$

Remark 1: The dynamics in (11) have been relaxed from the equality in (9) to ensure that the discrete problem is feasible, which will become clear in Proposition 1.

IV. PRELIMINARIES

We seek to address three questions related to solving the continuous-time optimal control (Problem 1) by solving the pseudospectral discretized constrained optimization (Problem 2). Suppose a feasible solution (x, u) exists to Problem 1. What are the conditions for:

1) ***Feasibility:*** For a given order of approximation, N, does Problem 2 have a feasible solution, $(\bar{x}, \bar{u})$, which are the interpolation coefficients given in (6) and (7)?
2) ***Convergence:*** As N increases, does the sequence of optimal solutions, $\{(\bar{x}^\dagger, \bar{u}^\dagger)\}$, to Problem 2 have a corresponding sequence of interpolating polynomials which converges to a feasible solution of Problem 1? Namely,
$$\lim_{N\to\infty} (\mathcal{I}_N x^\dagger, \mathcal{I}_N u^\dagger) = (x, u)$$
3) ***Consistency:*** As N increases, does the convergent sequence of interpolating polynomials corresponding to the optimal solutions of Problem 2 converge to an optimal solution of Problem 1? Namely,
$$\lim_{N\to\infty} (\mathcal{I}_N x^\dagger, \mathcal{I}_N u^\dagger) = (x^*, u^*)$$

The results in this section will provide the foundation on which we can analyze the feasibility, convergence, and consistency of the pseudospectral approximation method for optimal control problems. We begin by presenting several key established results in polynomial approximation theory and the natural vector extensions. With these inequalities, we are able then to prove feasibility and convergence. We define an optimal solution to Problem 1 as any feasible solution that achieves the optimal cost $J(x^*, u^*) = J^*$. We use this definition of an optimal solution within the subsequent preliminaries and the main result. To this end, the last lemma of this section introduces the error in the cost due to interpolation.

Remark 2: Note that $x \in H_n^\alpha(\Omega)$. Since $x(t)$ exists and $f \in C_n^{\alpha-1}$, all the derivatives $x^{(k)} \in C_n^0$, $\forall\ k = 0, 1, \dots, \alpha$ exist and are square integrable on the compact domain Ω, $x^{(k)} \in L_n^2(\Omega)$. Therefore, $x \in H_n^\alpha(\Omega)$.

Lemma 1 (Interpolation Error Bounds [8], p. 289): If $h \in H^\alpha(\Omega)$, the following hold with c_1, c_2, c_3, $c > 0$.

(a) The interpolation error is bounded,
$$\|h - \mathcal{I}_N h\|_2 \le c_1 N^{-\alpha} \|h\|_{(\alpha)}.$$

(b) The error between the exact derivative and the derivative of the interpolation is bounded,
$$\|\dot{h} - \mathcal{D}_N h\|_2 \le c_2 N^{1-\alpha} \|h\|_{(\alpha)}.$$
The same bound holds for the discrete $L^2(\Omega)$ norm,
$$\|\dot{h} - \mathcal{D}_N h\|_N \le c_3 N^{1-\alpha} \|h\|_{(\alpha)}.$$

(c) The error due to quadrature integration is bounded,

$$\left| \int_{-1}^{1} h(t)dt - \sum_{k=0}^{N} h(t_k) w_k \right| \leq c N^{-\alpha} \|h\|_{(\alpha)},$$

where t_k is the k^{th} LGL node and w_k is the corresponding k^{th} weight for LGL quadrature.

Lemma 2: If $h \in H_n^\alpha(\Omega)$, i.e., an n-vector valued Sobolev space, $h = (h_1\ h_2\ \ldots\ h_n)^T$, $h_i \in H^\alpha(\Omega)$, $i = 1, 2, \ldots, n$.

(a) The vector-valued extension of Lemma 1a is, by the triangular inequality on the $L_n^2(\Omega)$ norm,

$$\|h - \mathcal{I}_N h\|_2 \leq \sum_{i=1}^{n} \|h_i - \mathcal{I}_N h_i\|_2 \leq \sum_{i=1}^{n} c_i N^{-\alpha} \|h_i\|_{(\alpha)}.$$

(b) Similarly, 1b can be extended,

$$\begin{aligned}\|\dot{h} - \mathcal{D}_N h\|_2 &\leq \sum_{i=1}^{n} \|\dot{h} - \mathcal{D}_N h\|_2 \leq \sum_{i=1}^{n} c_i N^{1-\alpha} \|h_i\|_{(\alpha)} \\ &\leq c N^{1-\alpha},\end{aligned}$$

which again also holds for the discrete $L_n^2(\Omega)$ norm.

Proposition 1 (Feasibility): Given a solution (x, u) of Problem 1, then Problem 2 has a feasible solution, $(\bar{x}, \bar{u})$, which are the corresponding interpolation coefficients.

Proof: Given the feasible solution (x, u), let $(\mathcal{I}_N x, \mathcal{I}_N u)$ be the polynomial interpolation of this solution at the LGL nodes. Our aim is to show that the coefficients of this interpolation satisfy (11)-(13) of Problem 2. Consider the constraints imposed by the dynamics in (11). Because the discrete norm is evaluated only at the interpolation points,

$$\begin{aligned}\|f(\mathcal{I}_N x, \mathcal{I}_N u) - \mathcal{D}_N x\|_N &= \|f(x, u) - \mathcal{D}_N x\|_N \\ &= \|\dot{x} - \mathcal{D}_N x\|_N \\ &\leq c_d N^{1-\alpha}\end{aligned}$$

where the last step is given by Lemma 2b. Therefore, the interpolation coefficients $(\bar{x}, \bar{u})$ satisfy the dynamics of Problem 2 in (11). We can easily show that the path constraints are also satisfied because $g(x(t), u(t)) \leq 0$ for all $t \in \Omega$ by (4). Because this holds for all $t \in \Omega$, it also holds for all LGL nodes $t_k \in \Gamma^{\text{LGL}}$, i.e.,

$$g(\bar{x}_k, \bar{u}_k) = g(x(t_k), u(t_k)) \leq 0,$$

which gives (13). The endpoint constraints are trivially satisfied by the definition of interpolation and the presence of interpolation nodes at both endpoints. Therefore, $(\bar{x}, \bar{u})$ is a feasible solution to Problem 2. ■

Proposition 2 (Convergence): Given the sequence of solutions to Problem 2, $\{(\bar{x}, \bar{u})\}_N$, then the sequence of corresponding interpolation polynomials, $\{(\mathcal{I}_N x, \mathcal{I}_N u)\}$, has a convergent subsequence, such that

$$\lim_{N_j \to \infty} (\mathcal{I}_N x, \mathcal{I}_N u) = (\mathcal{I}_\infty x, \mathcal{I}_\infty u),$$

which is a feasible solution to Problem 1.

Proof: Given that $(\bar{x}, \bar{u})$ is a feasible solution of Problem 2, it satisfies (11)-(13). Our goal is to show that the sequence of polynomials, $\{(\mathcal{I}_N x, \mathcal{I}_N u)\}_N$, (i) is bounded, (ii) has a convergent subsequence and (iii) its limit is a feasible solution of Problem 1, satisfying (2)-(4).

(i) Explicitly writing out the discrete norm in (11) gives

$$\left(\sum_{k=0}^{N} \sum_{i=1}^{n} (f_i(\mathcal{I}_N x, \mathcal{I}_N u) - \mathcal{D}_N x_i)^2 (t_k) \right)^{1/2} \leq c_d N^{1-\alpha}.$$

Because f is continuous, it satisfies

$$\begin{aligned}\lim_{N \to \infty} \Big(f_i(\mathcal{I}_N x, \mathcal{I}_N u) - \mathcal{D}_N x_i \Big)(t_k) \qquad (15)\\ = \Big(f_i(\lim_{N \to \infty} \mathcal{I}_N x_i, \lim_{N \to \infty} \mathcal{I}_N u) - (\lim_{N \to \infty} \mathcal{I}_N x_i)' \Big)(t_k) \\ = 0,\end{aligned}$$

which means that the derivative of the interpolating polynomial and the state dynamics match at the interpolation nodes. Moreover, as $N \to \infty$, the LGL nodes $t_k \in \Gamma^{\text{LGL}}$ are dense in Ω, which shows that they match along the entire domain.

(ii) The sequence $\{\mathcal{I}_N x\}$ is a sequence of polynomials on the compact domain Ω, therefore, for each finite N, $\mathcal{I}_N x \in H_n^\alpha(\Omega)$. In the limit, we showed above in (15) that $(\lim_{N \to \infty} \mathcal{I}_N x)'$ matches the state dynamics $f \in C_n^{\alpha-1}$, so that $\{\mathcal{I}_N x\}$ are bounded, because f is bounded over Ω, and also satisfy $\mathcal{I}_N x \in H_n^\alpha(\Omega)$ for all N. With the boundedness of these interpolating polynomials $\{\mathcal{I}_N x\}$ all supported in Ω, Rellich's Theorem (cf., e.g., [10], p. 272) gives that there is a subsequence $\{\mathcal{I}_{N_j} x\}$ which converges in $H_n^{\alpha-1}(\Omega)$. The same is true for the control interpolating polynomial. Therefore, there exists at least one limit point of the function sequence $\{(\mathcal{I}_N x, \mathcal{I}_N u)\}$ which we denote $(\mathcal{I}_\infty x, \mathcal{I}_\infty u)$.

(iii) Because $\{\mathcal{I}_N x\}_N$ has a convergent subsequence, we can express (15) as

$$\frac{d}{dt}(\mathcal{I}_\infty x)(t_k) = f(\mathcal{I}_\infty x, \mathcal{I}_\infty u)(t_k), \qquad (16)$$

which states that $(\mathcal{I}_\infty x, \mathcal{I}_\infty u)$ satisfies the dynamics in (2) at the interpolation nodes. Again, as $N \to \infty$, the LGL nodes $t_k \in \Gamma^{\text{LGL}}$ are dense in Ω, which further shows that $(\mathcal{I}_\infty x, \mathcal{I}_\infty u)$ satisfies the dynamics of Problem 1 at all points on the interval Ω. Similarly, one can prove that this solution satisfies the path constraints because the LGL nodes become dense in Ω as $N \to \infty$ and $g(\bar{x}_k, \bar{u}_k) = g(x(t_k), u(t_k)) \leq 0$ at all LGL nodes. Again, the endpoint constraints are met exactly because the LGL grid has nodes at the endpoints. ■

Lemma 3: Given (x, u), where $x \in H_n^\alpha(\Omega)$ and $u \in H_m^\alpha(\Omega)$, and the corresponding interpolation coefficients, $(\bar{x}, \bar{u})$, then the error in the cost functionals defined in (1) and (10) due to interpolation is given by,

$$|J(x, u) - \bar{J}(\bar{x}, \bar{u})| \leq c N^{-\alpha}.$$

Remark 3: Notice that (x, u) and $(\bar{x}, \bar{u})$ are not required to be a feasible solutions to Problem 1 and 2, respectively. This result characterizes the error due to interpolation.

Proof: From (2) and (11) since $\varphi(x(1)) = \varphi(\bar{x}_N)$,

$$|J(x,u) - \bar{J}(\bar{x},\bar{u})| = \left| \int_{-1}^{1} \mathcal{L}(x,u)dt - \sum_{k=0}^{N} \mathcal{L}(\bar{x}_k,\bar{u}_k)w_k \right|.$$

Since $\mathcal{L} \in C^\alpha$, $x \in H_n^\alpha(\Omega)$, and $u \in H_m^\alpha(\Omega)$, the composite function $\tilde{\mathcal{L}}(t) = \mathcal{L}(x(t),u(t)) \in H^\alpha(\Omega)$. Let $\mathcal{L}_k = \mathcal{L}(\bar{x}_k,\bar{u}_k)$. Substituting these definitions and employing Lemma 1c, we obtain

$$\left| \int_{-1}^{1} \tilde{\mathcal{L}}(t)dt - \sum_{k=0}^{N} \mathcal{L}_k w_k \right| \le cN^{-\alpha}\|\tilde{\mathcal{L}}(t)\|_{(\alpha)}.$$

Because $\tilde{\mathcal{L}} \in H^\alpha(\Omega)$, $\|\tilde{\mathcal{L}}(t)\|_{(\alpha)}$ is finite, from which the result follows. ■

V. MAIN RESULT

Theorem 1 (Consistency): Suppose Problem 1 has an optimal solution (x^*,u^*). Given a sequence of optimal solutions to Problem 2, $\{(\bar{x}^\dagger,\bar{u}^\dagger)\}_N$, then the corresponding sequence of interpolating polynomials, $\{(\mathcal{I}_N x^\dagger,\mathcal{I}_N u^\dagger)\}_N$, has a limit point, $(\mathcal{I}_\infty x^\dagger,\mathcal{I}_\infty u^\dagger)$ which is an optimal solution to the original optimal control problem.

Proof: We break the proof into four sections, employing the results from the previous section.

(i) By Proposition 1, since (x^*,u^*) is a solution to Problem 1, then for each choice of N, the corresponding interpolation coefficients, $(\bar{x}^*,\bar{u}^*)$, are a feasible solution to Problem 2. By the definition of optimality of $(\bar{x}^\dagger,\bar{u}^\dagger)$,

$$\bar{J}(\bar{x}^\dagger,\bar{u}^\dagger) \le \bar{J}(\bar{x}^*,\bar{u}^*). \tag{17}$$

(ii) By Proposition 2, the limit point of the polynomial interpolation of the discrete optimal solution to Problem 2, $\lim_{N\to\infty}(\mathcal{I}_N x^\dagger,\mathcal{I}_N u^\dagger) = (\mathcal{I}_\infty x^\dagger,\mathcal{I}_\infty u^\dagger)$, is a feasible solution of Problem 1. Therefore, we have, by the definition of the optimality of (x^*,u^*) and the continuity of J,

$$\begin{aligned} J(x^*,u^*) &\le \lim_{N\to\infty} J(\mathcal{I}_N x^\dagger,\mathcal{I}_N u^\dagger) \\ &= J(\mathcal{I}_\infty x^\dagger,\mathcal{I}_\infty u^\dagger). \end{aligned} \tag{18}$$

(iii) Using Lemma 3, we can bound the error in the cost between the optimal solution of Problem 1, (x^*,u^*), and the corresponding interpolating coefficients, $(\bar{x}^*,\bar{u}^*)$, as

$$|J(x^*,u^*) - \bar{J}(\bar{x}^*,\bar{u}^*)| \le c_1 N^{-\alpha}. \tag{19}$$

Similarly, we can bound the error in the cost between the optimal solution of Problem 2, $(\bar{x}^\dagger,\bar{u}^\dagger)$, and the polynomial interpolation of this solution, $(\mathcal{I}_N x^\dagger,\mathcal{I}_N u^\dagger)$, as

$$|J(\mathcal{I}_N x^\dagger,\mathcal{I}_N u^\dagger) - \bar{J}(\bar{x}^\dagger,\bar{u}^\dagger)| \le c_2 N^{-\alpha}. \tag{20}$$

Recall that Lemma 3 does not require $(\mathcal{I}_N x^\dagger,\mathcal{I}_N u^\dagger)$ to be a feasible solution of Problem 1. From (19) and (20),

$$\lim_{N\to\infty} \bar{J}(\bar{x}^*,\bar{u}^*) = J(x^*,u^*), \tag{21}$$

$$\lim_{N\to\infty} \left[J(\mathcal{I}_N x^\dagger,\mathcal{I}_N u^\dagger) - \bar{J}(\bar{x}^\dagger,\bar{u}^\dagger)\right] = 0. \tag{22}$$

(iv) We are now ready to assemble the various pieces of this proof. Combining (21) and (17) we have,

$$\lim_{N\to\infty} \bar{J}(\bar{x}^\dagger,\bar{u}^\dagger) \le \lim_{N\to\infty} \bar{J}(\bar{x}^*,\bar{u}^*) = J(x^*,u^*).$$

Adding the result from (18),

$$\lim_{N\to\infty} \bar{J}(\bar{x}^\dagger,\bar{u}^\dagger) \le J(x^*,u^*) \le \lim_{N\to\infty} J(\mathcal{I}_N x^\dagger,\mathcal{I}_N u^\dagger). \tag{23}$$

Since the difference between the left and right sides, as given by (22), decreases to zero as $N\to\infty$, the quantities $\bar{J}(\bar{x}^\dagger,\bar{u}^\dagger)$ and $J(\mathcal{I}_N x^\dagger,\mathcal{I}_N u^\dagger)$ converge to $J(x^*,u^*)$, i.e.,

$$\begin{aligned} 0 &\le \lim_{N\to\infty} \left[J(x^*,u^*) - \bar{J}(\bar{x}^\dagger,\bar{u}^\dagger)\right] \\ &\le \lim_{N\to\infty} \left[J(\mathcal{I}_N x^\dagger,\mathcal{I}_N u^\dagger) - \bar{J}(\bar{x}^\dagger,\bar{u}^\dagger)\right] = 0. \end{aligned}$$

Thus the optimal discrete cost $\bar{J}(\bar{x}^\dagger,\bar{u}^\dagger)$ of Problem 2 and the continuous cost $J(\mathcal{I}_N x^\dagger,\mathcal{I}_N u^\dagger)$ of the corresponding interpolation polynomials converge to the optimal cost $J(x^*,u^*)$ of Problem 1. Moreover, $(\mathcal{I}_\infty x^\dagger,\mathcal{I}_\infty u^\dagger)$ is a feasible solution to Problem 1 and achieves the optimal cost. Therefore, $(\mathcal{I}_\infty x^\dagger,\mathcal{I}_\infty u^\dagger)$ is an optimal solution to Problem 1. ■

VI. ENSEMBLE EXTENSION

Ensemble Control pertains to the study of a continuum of dynamical systems of the form [11], [12],

$$\frac{d}{dt}x(t,s) = f\big(t,s,x(t,s),u(t)\big), \tag{24}$$

which is indexed by a parameter vector that exhibits variation within an interval, $s \in \mathcal{S} \subset \mathbb{R}^d$ but controlled by the open loop input $u(t)$. Such systems arise from environmental interactions, uncertainty, or inherent variability that induces inhomogeneity in the characteristic parameters of the dynamics. An optimal ensemble control problem is formulated by replacing the dynamics with the ensemble dynamics in (24) and the cost with,

$$J = \Big(\int_{\mathcal{S}} \varphi(x(1,s)) + \int_{-1}^{1} \mathcal{L}(x(t,s),u(t))dt\Big)ds, \tag{25}$$

and the end and path constraints are extended in a straightforward manner. The method employs $d+1$ dimensional interpolating polynomials to represent x and u with the approximate dynamics (compare to (9)) given by [4],

$$\frac{d}{dt}I_{N\times N_{s_1}\times\cdots\times N_{s_d}}x(t,\mathbf{s_j}) = \sum_{k=0}^{N} D_{ik}\bar{x}_{kj_1\ldots j_d}, \tag{26}$$

where $\mathbf{s} = (s_1,s_2,\ldots,s_d)' \in \mathcal{S} \subset \mathbb{R}^{\mathrm{d}}$. This extension hinges upon the lack of time dependence in the new dimensions of the problem (d parameter dimensions). Propositions 1 and 2 can then be extended in a straightforward manner by incorporating additional dynamics constraints that act in parallel. Lemma 3 will include gaussian quadrature approximations of both the s and t integrals. With these limited modifications, the approach above guarantees the convergence of the multidimensional pseudospectral method applied to optimal ensemble control problems.

VII. EXAMPLES

In this section we demonstrate the multidimensional pseudospectral method and the convergence of the method through examples from quantum control and neuroscience.

A. POLARIZATION TRANSFER IN NMR

Polarization transfer is an important fundamental technique used in NMR spectroscopy to reveal the structure of complex biomolecules and has far-reaching impacts on our understanding of, e.g., cell signaling and drug delivery. Optimal control techniques have achieved significant advancements in pulse design, which in turn yield increased efficiencies in polarization transfer [13], [2], [3]. Physical models of this transfer contain parameters that are perturbed by the chemical environment surrounding the system. It is possible for the spin coupling variation to be on the same order as the value of the nominal coupling, for example 5-13 Hz in a HNC_α protein. Recent studies of such ensemble polarization transfer have used an optimal control formulation given by,

$$\begin{aligned} \max \quad & \eta = \frac{1}{2\delta J}\int_{1-\delta J}^{1+\delta J} x_6(T,J)\ dJ \\ \text{s.t.} \quad & \begin{bmatrix} \dot{x}_1 \\ \dot{x}_2 \\ \dot{x}_3 \\ \dot{x}_4 \\ \dot{x}_5 \\ \dot{x}_6 \end{bmatrix} = \begin{bmatrix} 0 & -u_1 & u_2 & 0 & 0 & 0 \\ u_1 & -\xi_a & -0 & -J & -\xi_c & 0 \\ -u_2 & 0 & -\xi_a & -\xi_c & J & 0 \\ 0 & J & -\xi_c & -\xi_a & 0 & -u_2 \\ 0 & -\xi_c & -J & -0 & -\xi_a & u_1 \\ 0 & 0 & 0 & u_2 & -u_1 & 0 \end{bmatrix} \begin{bmatrix} x_1 \\ x_2 \\ x_3 \\ x_4 \\ x_5 \\ x_6 \end{bmatrix}, \\ & x(0,J) = [1\ 0\ 0\ 0\ 0\ 0]', \\ & \sqrt{u_1^2(t)+u_2^2(t)} \le A,\ \forall t \in [0,T], \end{aligned} \tag{27}$$

where the transfer efficiency (cost) η maximizes the value of x_6 over the ensemble at the terminal time T; x_i are expectation values of components of the spin operators; $J \in [1-\delta J, 1+\delta J]$, $\delta J \in (0,1)$, is the scalar coupling between spins exhibiting variation; ξ_a and ξ_c are autocorrelated and cross-correlation relaxation rates, respectively; u_1 and u_2 are the applied pulses (controls); and A is the maximum allowable amplitude [2]. The dynamics and parameters are normalized by a nominal scalar coupling J_0.

Figure 1 displays the convergence of the multidimensional pseudospectral method as the order of approximation, N, increases and corresponding to solutions of (27) with a 30 Hz variation around the nominal scalar coupling $J_0 = 93$ Hz ($\delta J = 30/93 \approx 0.32$ in the normalized case). The analytically derived optimal transfer efficiency of a single-valued system (i.e., δJ=0), denoted as CROP [13], is plotted as an upper bound on the expected efficiency for the ensemble case. As a dissipative system, the ensemble case is not expected to fully compensate for the ensemble variation, but achieves a more uniform transfer efficiency with a small error from this upper bound. Consideration of the ensemble control problem as in (27) is motivated by the efficiency corresponding to a single-valued optimization (gray dashed line in Figure 1), which performs well at the nominal parameter value, but degraded performance at the edges.

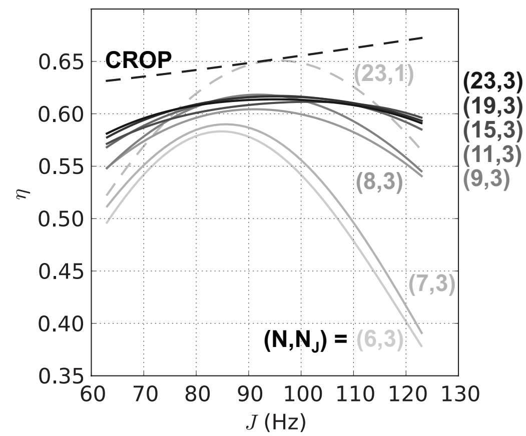

Fig. 1. A series of solutions to the problem of polarization transfer achieved by the multidimensional pseudospectral method. The level of discretization, N is increased illustrating the rapid convergence characteristic of the pseudospectral method. The analytically derived optimal transfer efficiency for the single-valued system, CROP [13], provides an upper bound on the expected ensemble efficiency. A single-valued pseudospectral optimized solution (gray dashed line) achieves a narrow window of performance with degraded performance on the edges of the variation, which prompts us to specifically consider the ensemble variation. (Parameters: $J \in [63, 123]$ Hz, $\xi_a = 183$ Hz, $\xi_c = 163$ Hz, $T = 25$ms, A=50 Hz)

B. SPIKING OF NEURON OSCILLATORS

The dynamic interactions of neurons in the human brain are often modeled as a network of weakly connected nonlinear oscillators [14]. Each individual neuron can be modeled by a system $\dot{x} = f(x, I, \alpha)$ with an attractive, non-constant, periodic limit cycle, where $x(t) \in \mathbb{R}^n$, $I(t) \in \mathbb{R}$, and $\alpha \in \mathbb{R}^p$ are the state, control, and parameter set, respectively. This can be reduced to a scalar system, called a phase model, of the form $\dot{\theta} = \omega(\alpha) + Z(\theta, \alpha)I$, where $\theta(t)$ is a phase variable that represents the position of $x(t)$ near the limit cycle, $\omega(\alpha)$ is the natural frequency, $I(t)$ is the control, and the phase response curve (PRC) $Z(\theta, \alpha)$ is a 2π-periodic function of θ, which quantifies the shift in θ due to an infinitesimal perturbation in x [15]. The reduction is valid for bounded input, i.e. $|I| \le A$, and provides a theoretical basis for controlling the spiking period of a neuron [5] where the objective of minimum control power arises from physiological considerations. In an experimental or clinical setting, it is often desirable to synchronize the spiking period T of a collection of neurons, each of which has a slightly different PRC due to variation in the parameters α over a given range. We formulate this as an optimal ensemble control problem steering $\theta(0) = 0$ to $\theta(T) = 2\pi$,

$$\begin{aligned} \min \quad & \eta = \int_0^T I^2(t)\ dt \\ \text{s.t.} \quad & \dot{\theta} = \omega(\alpha) + Z(\theta, \alpha)I, \\ & |I| \le A,\ \forall t \in [0,T],\ \ \alpha \in D \subset \mathbb{R}^p \end{aligned} \tag{28}$$

where D is an interval containing a nominal parameter α_0.

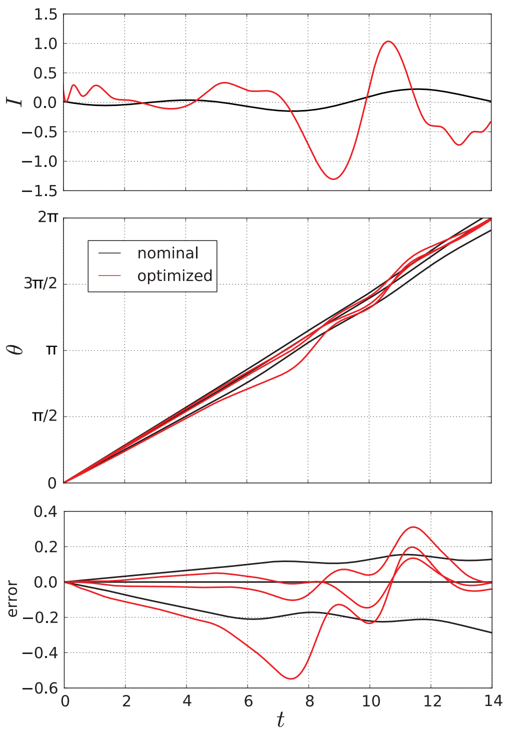

Fig. 2. Solutions to the neuron phase model using a Fourier representation of the PRC. The control inputs (top) were generated by considering the nominal and ensemble cases individually. The corresponding state trajectories (middle) of a 3-neuron ensemble show divergence and convergence of the states following the nominal and ensemble control, respectively. The difference between the nominal trajectory following the nominal control and each of the other state trajectories (bottom) shows the compensating behavior of the ensemble input more clearly. (Parameters: $\overline{g}_{Na} = 120$ mS/cm$^2 \pm 10\%$)

Consider the Hodgkin-Huxley model, which describes the propagation of action potentials in a squid axon, and is a canonical example of neural oscillator dynamics [16], with a nominal spiking period $\tau_0 = 14.638$. Suppose that we wish to synchronize the spiking of neurons to period $\tau = 14$ when sodium conductance $\overline{g}_{Na}$ varies on the interval $[108, 132]$ mS/cm^2, with nominal value 120 mS/cm^2. From the PRCs for the nominal and extreme cases shown in Figure 3, we see that the variation is significant, and indeed the spiking period $\tau = 2\pi/\omega(\alpha)$ varies from 14.070 to 15.971. The optimal ensemble control method is applied to solve (28) for this example, where $\alpha = \overline{g}_{Na}$ is a scalar sampled at LGL nodes, and the PRCs are represented using a Fourier approximation for the computation. Figure 2 shows the computed optimal control, the trajectories, and the difference between the solutions and the nominal trajectory. When the nominal control is applied, the phases of the neurons drift apart, but when the optimal ensemble control is applied, the phases cluster near $\theta = 2\pi$ at $t = T = \tau = 14$, as desired.

VIII. CONCLUSION

The pseudospectral method and the more recent multi-dimensional pseudospectral method are effective computational methods to solve challenging optimal control problems on complex systems. Here we consolidate and extend the current results on the convergence of these methods. Characterizing the conditions of convergence is key to understanding the abilities and limitations of the approach as well as to establish the credibility of the solutions generated with the methods. We provide examples to illustrate the technique and motivate the convergence results empirically.

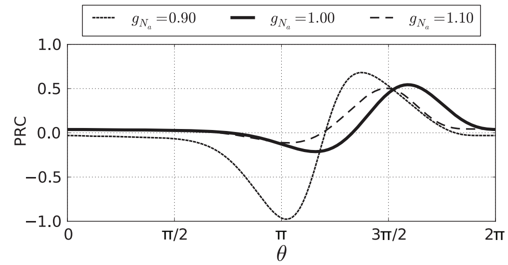

Fig. 3. The Fourier representation of the phase response curves corresponding to the ensemble in Figure 2. Although the origin of the parameter variation is small the PRC shifts dramatically.

REFERENCES

[1] Q. Gong, M. Ross, W. Kang, F. Fahroo, Connections between the covector mapping theorem and convergence of the pseudospectral method for optimal control, *Comput. Optim. Appl*, 41, 2008, pp. 307-335.

[2] J.-S. Li, J. Ruths, and D. Stefanatos, A pseudospectral method for optimal control of open quantum systems, *J. Chem. Phys.*, vol. 131, 2009, pp. 164110.

[3] J. Ruths, J.-S. Li. Optimal ensemble control of open quantum systems with a pseudospectral method, *49th IEEE CDC*, Atlanta, 2010.

[4] J. Ruths and J.-S. Li, A multidimensional pseudospectral method for optimal control of quantum ensembles, *J. Chem. Phys.*, 134, 2011, pp. 044128.

[5] J.-S. Li, Control of a network of spiking neurons, *8th IFAC Symposium on Nonlinear Control Systems*, Italy, Sep. 2010.

[6] Q. Gong, W. Kang, M. Ross, A pseudospectral method for the optimal control of constrained feedback linearizable systems, *IEEE Trans. Autom. Control*, 51, 2006, pp. 1115.

[7] G. Szego, *Orthogonal Polynomials*, American Mathematical Society, New York, 1959.

[8] C. Canuto, M. Y. Hussaini, A. Quarteroni and T. A. Zang, *Spectral Methods*, Springer, Berlin, 2006.

[9] J. Boyd, *Chebyshev and Fourier Spectral Methods*, Dover Ed. 2, New York, 2000.

[10] G. B. Folland, *Real Analysis: Modern Techniques and Their Applications*, John Wiley & Sons, New York, 1984.

[11] J.-S. Li and N. Khaneja, Ensemble control of Bloch equations, *IEEE Trans. Autom. Control*, vol. 54, 2009, pp. 528-536.

[12] J.-S. Li, Ensemble control of finite-dimensional time-varying linear systems, *IEEE Trans. Autom. Control*, vol. 56, 2011, pp. 345-357.

[13] N. Khaneja, B. Luy, and S. J. Glaser, Boundary of quantum evolution under decoherence, *Proc. Natl. Acad. Sci. USA*, vol. 100, 2003, pp. 13162-13166.

[14] F. Hoppensteadt and E. Izhikevich, *Weakly connected neural networks*, Springer-Verlag, New Jersey, 1997.

[15] E. Brown, J. Moehlis, and P. Holmes, On the Phase Reduction and Response Dynamics of Neural Oscillator Populations, *Neural Computation*, vol. 16, 2004, pp. 673-715.

[16] A. Hodgkin and A. Huxley, A quantitative description of membrane current and its application to conduction and excitation in nerve, *The Journal of Physiology*, vol. 117, 1952, pp. 500-544.